# Structures of Vinylstannane (Ethenylstannane) and Allylstannane (2-Propenylstannane) Determined by Gas-Phase Electron Diffraction and Quantum Chemical Calculations

Tatyana Strenalyuk,[†] Svein Samdal,*[,†] Harald Møllendal,[†] and Jean-Claude Guillemin[‡]

*Department of Chemistry, University of Oslo, Post Office Box 1033 Blindern, NO-0315 Oslo, Norway, and Sciences Chimiques de Rennes, Unite Mixte de Recherche 6226 CNRS-ENSCR, Ecole Nationale Supérieure de Chimie de Rennes, F-35700 Rennes, France*

*Received February 17, 2006*

Vinylstannane ($H_2C{=}CHSnH_3$) and allylstannane ($H_2C{=}CHCH_2SnH_3$) have been synthesized, and their structures and conformational properties have been determined by ab initio and density functional theory calculations and gas electron diffraction. There is only one stable conformation of vinylstannane, where one of the Sn−H bonds is *synperiplanar* to the double bond. The most important structural parameter is the C($sp^2$)−Sn(IV) bond length, which is $r_a = 215.1(6)$ pm ($r_e = 214.1(6)$ pm). The CCSn bond angle is 121.6(4)°. Uncertainties are estimated errors equal to 2.5 times the least-squares standard deviation and include uncertainty in the electron wavelength. Theoretical calculations indicate that there are two stable rotameric forms of allystannane. The C=C−C−Sn chain of atoms is *synperiplanar* (dihedral angle = 0°) in the less stable form and *anticlinal* (dihedral angle ≈ 106° from *synperiplanar*) in the more stable rotamer. Theoretical calculations predict an energy difference between the two conformations of about 10 kJ $mol^{-1}$. There is no indication of the presence of the *synperiplanar* conformation in the gas phase at room temperature. The final analysis was therefore carried out assuming that only the *anticlinal* conformer was present. The C=C−C−Sn dihedral angle was found to be 102.9(19)° from the *synperiplanar* conformer, which is the smallest value found for this angle in the C=C−C−X (X = C, Si, Ge, Sn) series of compounds. The C($sp^3$)−Sn(IV) bond length is $r_a = 218.9(8)$ pm ($r_e = 217.6(8)$ pm), and the CCSn bond angle is 110.9(6)°. The B3LYP calculations using the cc-pVTZ basis set for C and H and the cc-pVTZ-PP basis set for Sn reproduce the experimental $r_e$(C−Sn) bond distances very well, while the MP2(FC) calculations underestimate the $r_e$(C−Sn) bond distances by 3−4 pm.

## Introduction

Progress made in the last decade toward the synthesis of primary α,β- and β,γ-unsaturated stannanes (e.g., allenylstannane,[1] 1-alkynylstannane,[1] and propargylstannane[2]) makes it possible to study the molecular properties of the smallest members of these compounds. The geometrical structures of these smallest stannanes are important because they will serve as prototypes for this family of molecules and act as reference structures when the molecular structures of larger stannanes are discussed. Moreover, it will also be important to know the molecular structure in the gas phase when comparisons are made with the structures in the condensed phase in order to assess the influence of intermolecular forces. Accurate molecular geometries of these prototypes are useful for quantum chemists exploring computational methods and basis sets.

Vinylstannane ($H_2C{=}CHSnH_3$) is the smallest stannane with a double bond and is therefore of special interest. Recently, a first determination of a Sn−C($sp^2$) bond distance[3] has been determined in the gas phase for a free allenylstannane ($H_2C{=}C{=}CHSnH_3$) molecule. A comparison of the Sn−C($sp^2$) bond distances in vinylstannane and allenylstannane would be interesting to see if the C=C=C group will have any effect on the Sn−C($sp^2$) bond distance.

Allylstannane ($H_2C{=}CH{-}CH_2SnH_3$) is the smallest unsaturated stannane that can exist as a conformational mixture. To our knowledge, very little information is available about the conformational behavior of these molecules. The present study of allylstannane should therefore be of interest.

Gas electron diffraction (GED) is a well-suited method to investigate the conformational and structural problems presented by vinyl- and allylstannane. The scarcity of information concerning the molecular structures and conformational properties of unsaturated organostannanes in general was the motivation to undertake the present investigation.

## Synthesis of Vinyl- and Allylstannane

The preparation of several 1-alkenylstannanes has already been reported.[4,5] In 1959, Brinckman and Stone[4] reported the first synthesis of the unsubstituted derivative, vinylstannane **1**, by addition of lithium aluminum hydride (LAH) to trichloroethenylstannane **2**.[6,7] Compound **1** was obtained in a low yield

* Corresponding author. E-mail: svein.samdal@kjemi.uio.no. Tel: 47 2285 5458. Fax: +47 2285 5441.

[†] University of Oslo.

[‡] Ecole Nationale Supérieure de Chimie de Rennes.

(1) Lassalle, L.; Janati, T.; Guillemin, J.-C. *J. Chem. Soc., Chem. Commun.* **1995**, 699.

(2) Guillemin, J.-C.; Malagu, K. *Organometallics* **1999**, *18*, 5259.

(3) Strenalyuk, T. S.; Samdal, S.; Møllendal, H.; Guillemin, J.-C. *Organometallics*, in press.

(4) Brinckman, F. E.; Stone, F. G. A. *J. Inorg., Nucl. Chem.* **1959**, *11*, 24.

(5) Janati, T.; Guillemin, J.-C.; Soufiaoui, M. *J. Organomet. Chem.* **1995**, *486*, 57.

(6) Seyferth, D.; Stone, F. G. A. *J. Am. Chem. Soc.* **1957**, *79*, 515.

(7) Rosenberg, S. D.; Gibbons, A. J., Jr.; Ramsden, H. E. *J. Am. Chem. Soc.* **1957**, *79*, 2137.

10.1021/om0601549 CCC: $33.50 
Publication on Web 04/04/2006

**Scheme 1**

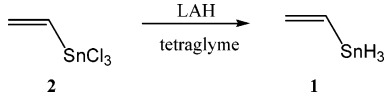


2 1

**Scheme 2**

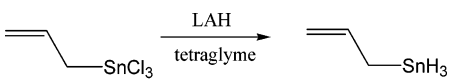


4 3

after a difficult purification. This approach was then optimized and generalized to substituted derivatives (Scheme 1).[5]

Only one allylic stannane with Sn−H bonds, the (*E*)-but-2-enyldimethylstannane, has so far been prepared.[8] The unsubstituted derivative, 2-propenylstannane **3**, was synthesized in Rennes by reduction of trichloro-2-propenylstannane **4** with LAH. Allylstannane **3** was obtained in a 34% yield and characterized by infrared and $^1$H, $^{13}$C, and $^{119}$Sn NMR spectroscopy and high-resolution mass spectrometry (HRMS). The $^1$H NMR chemical shifts and coupling constants are typical for allylstannane, and the $^{119}$Sn NMR chemical shift ($\delta$ −328.9 ppm) is comparable to that of phenylstannane ($\delta$ −320 ppm) and the low-frequency shift relative to those of primary alkylstannanes ($EtSnH_3$: $\delta$ −282 ppm).[5] The half-life time of a 5% sample diluted in deuterotoluene or $CD_2Cl_2$ is about 6 h, and it increases to 1 day in the presence of duroquinone, a radical inhibitor. Brown, unidentified oligomeric compounds were obtained on standing at room temperature.

## Experimental Section

**Materials.** Tetraglyme, lithium aluminum hydride, 2-propenyltri-*n*-butylstannane, and tin tetrachloride were purchased from Aldrich and used without further purification. Trichloroethenylstannane **2** has been prepared as previously reported.[6,7]

**Preparation of Ethenylstannane 1.** The apparatus previously described for the reduction of phosphonates[9] was used. A 250 mL flask containing the reducing mixture (1.6 g, 40 mmol of $LiAlH_4$ in 60 mL of tetraglyme) was attached to the vacuum line, cooled to −10 °C, and degassed. The trichloroethenylstannane **2** (5.0 g, 20 mmol in 20 mL of tetraglyme) was slowly added with a flex-needle through the septum. During and after the addition, the high-boiling compounds were removed in a trap cooled at −80 °C, and ethenylstannane **1** was condensed in a second trap cooled at −130 °C. When the reaction was complete (30 min), the second trap was disconnected from the vacuum line by stopcocks, attached to the spectrometer, and kept at a low temperature (−80 °C) before analysis. Ethenylstannane **1** was obtained in 63% yield (1.9 g, 12.6 mmol).

**2-Propenyltrichlorostannane 4.**[10−13] Into a 50 mL two-necked flask immersed in a cold bath (−30 °C) and equipped with a magnetic stirring bar and through a nitrogen inlet was introduced tin tetrachloride (13.1 g, 50 mmol). 2-Propenyltri-*n*-butylstannane (16.5 g, 50 mmol) was added dropwise for about 5 min. The mixture was allowed to warm to 30 °C and stirred for 20 min at this temperature. The product purified by distillation (bp 51 °C (0.1 mm of Hg)) was obtained in a 67% yield (8.9 g, 33 mmol).

**2-Propenylstannane 3.** The apparatus used for ethenylstannane **1** was employed. A 250 mL flask containing the reducing mixture (1.6 g, 40 mmol of $LiAlH_4$ in 60 mL of tetraglyme) was attached to the vacuum line, cooled to −10 °C, and degassed. The 2-propenyltrichlorostannane **4** (2.66 g, 10 mmol in 20 mL of tetraglyme) was then slowly added (10 min) via a flex-needle through a septum. During and after the addition, the 2-propenylstannane **3** was distilled off in vacuo from the reaction mixture. A cold trap (−80 °C) selectively removed the less volatile products, and stannane **3** was condensed into a cell cooled at −120 °C. After being disconnected from the vacuum line by stopcocks, the cell was connected to the spectrometer and kept at low temperature (< −80 °C) before analysis. $Bp_{0.1} \approx -90$ °C. Yield: 34%. $\tau_{1/2}$ (5% diluted in $C_7D_8$ or $CD_2Cl_2$, room temperature): 6 h. $^1$H NMR ($C_7D_8$): $\delta$ 1.61 (d, 2H, $^3J_{HH} = 8.3$ Hz, $^2J_{^{119}SnH} = 74.0$ Hz, $CH_2Sn$); 4.36 (t, 3H, $^3J_{HH} = 2.0$ Hz, $^1J_{^{119}SnH} = 1855$ Hz, $SnH_3$); 4.63 (d, 1H, $^3J_{HHcis} = 9.9$ Hz, $^4J_{^{119}SnH} = 28.0$ Hz, C=C*H*(H)); 4.74 (d, 1H, $^3J_{HHtrans} = 16.7$ Hz, $^4J_{^{119}SnH} = 29.0$ Hz, C=CH(*H*)); 5.68 (ddt, 1H, $^3J_{HHtrans} = 16.7$ Hz, $^3J_{HHcis} = 9.9$ Hz, $^3J_{HH} = 8.3$ Hz, CH). $^{13}$C NMR ($C_6D_6$): $\delta$ 11.6 (t, $^1J_{CH} = 133.3$ Hz, $^1J_{^{119}SnC} = 354.2$ Hz (d)); 112.1 (dd, $^1J_{CH} = 153.4$ Hz, $^1J_{CH} = 160.6$ Hz, $^3J_{^{119}SnC} = 61.8$ Hz (d)); 137.4 (d, $^1J_{CH} = 151.8$ Hz, $^2J_{^{119}SnC} = 55.4$ Hz (d)). $^{119}$Sn NMR ($C_6D_6$−$C_7H_8$, rt): $\delta$ −328.9 ($^1J_{^{119}SnH} = 1855$ Hz). Gas-phase IR ($\nu_{cm^{-1}}$): 3091 (m, $\nu_{C=CH}$), 2983 (m), 2928 (m), 1904 (vs, $\nu_{Sn-H}$), 1634 (m, $\nu_{C=C}$), 1194 (w), 1027 (w), 901 (m), 682 (s). HRMS: calcd for $C_3H_8{}^{120}Sn$ 163.9648, found 163.964.

**Microwave Experiment.** Attempts were also made to observe the microwave spectrum of vinylstannane in the 26−62 GHz spectral interval using the Oslo Stark spectrometer.[14] However, no signals that could be attributed to vinylstannane were observed. Since the intensities of the spectral transitions are proportional to the square of the dipole moment, the failure to observe a spectrum is assumed to indicate that the dipole moment of this compound is too small. This is consistent with the quantum chemical predictions described below.

**Electron-Diffraction Experiment.** Vinylstannane and allylstannane were synthesized in Rennes as described above, and the purity was determined by $^1$H NMR spectroscopy to be 97 and 92%, respectively. The same syntheses were performed in Oslo without any further checking of the purity. The compounds were pumped on before exposure to remove the most volatile components. Both compounds were distilled directly into the apparatus. The estimated purity should therefore be better than stated above. The sample bulb was partially in liquid $N_2$ and adjusted to give a steady gas flow through the nozzle in order to get optimum scattering conditions. Neither the vapor pressure nor the temperature inside the sample bulb was monitored during the experiment.

GED data were recorded using a Balzers KD-G2 unit.[15] The experimental data were recorded on BAS-III image plates, which were scanned using a BAS-1800II scanner. Both the image plates and the scanner are manufactured by FujiFilm.

Each image plate was divided into four sectors, two in the *x*-direction (left and right) and two in the *y*-direction (up and down). Data for each sector were treated separately, and the two sectors in the *x*-direction were averaged to give one modified intensity curve in the *x*-direction and, similarly, one modified intensity curve in the *y*-direction. The data range in *x*- and *y*-direction is slightly different, as a consequence of the rectangular shape of the image plate. This procedure applies for both camera distances and gave four curves as shown in Figures 4 and 6. These four curves were

(8) Clark, H. C.; Kwon, J. T. *Can. J. Chem.* **1964**, *42*, 1288.
(9) Demaison, J.; Guillemin, J.-C.; Møllendal, H. *Inorg. Chem.* **2001**, *40*, 3719.
(10) Fishwick, M.; Wallbridge, M. G. H. *J. Organomet. Chem.* **1970**, *25*, 69.
(11) Naruta, Y.; Nishigaichi, Y.; Maruyama, K. *Tetrahedron* **1989**, *45*, 1067.
(12) Denmark, S. E.; Wilson, T.; Willson, T. M. *J. Am. Chem. Soc.* **1988**, *110*, 984.
(13) Thoonen, S.; Deelman, B.-J.; van Koten, G. *Tetrahedron* **2003**, *59*, 10261.
(14) Møllendal, H.; Leonov, A.; de Meijere, A. *J. Phys. Chem. A* **2005**, *109*, 6344.
(15) Zeil, W.; Haase, J.; Wegmann, L. *Z. Instrumentenk.* **1966**, *74*, 84.

**Table 1. Experimental Conditions of the GED Investigation**

| | vinylstannane | | allylstannane | |
|---|---|---|---|---|
| camera distance/mm | 498.65 | 248.88 | 498.65 | 248.88 |
| electron wavelength/pm | 5.820 | 5.820 | 5.820 | 5.820 |
| nozzle temperature/°C | 22 | 22 | 22 | 22 |
| s ranges/nm$^{-1}$: *x*-direction | 20.00−145.00 | 40.00−270.00 | 22.25−148.75 | 50.00−290.00 |
| *y*-direction | 20.00−131.25 | 40.00−250.00 | 20.00−130.00 | 50.00−240.00 |
| $\Delta s$/nm$^{-1}$ | 1.25 | 2.50 | 1.25 | 2.50 |

**Table 2. Calculated Structure[a] of Vinylstannane ($C_s$-symmetry)**

| | HF[b] | | B3LYP[b] | | MP2[b] (FC) |
|---|---|---|---|---|---|
| | *sp* | *ap* | *sp* | *ac* | *sp* |
| | | | Bond Lengths | | |
| $Sn_1-C_2$ | 213.8 | 214.2 | 214.6 | 215.1 | 211.2 |
| $C_2=C_3$ | 132.0 | 131.9 | 132.8 | 132.8 | 133.9 |
| $Sn_1-H_7$ | 171.2 | 171.2 | 171.5 | 171.5 | 169.0 |
| $Sn_1-H_8$ | 171.3 | 171.2 | 171.7 | 171.6 | 169.1 |
| $C_2-H_6$ | 107.8 | 107.8 | 108.6 | 108.6 | 108.4 |
| $C_3-H_4$ | 107.7 | 107.7 | 108.6 | 108.6 | 108.4 |
| $C_3-H_5$ | 107.6 | 107.7 | 108.4 | 108.5 | 108.3 |
| | | | Bond Angles | | |
| $\angle Sn_1C_2C_3$ | 123.4 | 124.4 | 123.4 | 124.4 | 122.3 |
| $\angle C_3C_2H_6$ | 117.9 | 117.8 | 118.8 | 118.6 | 117.6 |
| $\angle C_2C_3H_4$ | 121.9 | 121.9 | 121.8 | 121.8 | 121.7 |
| $\angle C_2C_3H_5$ | 122.5 | 122.7 | 122.5 | 122.8 | 121.9 |
| $\angle C_2Sn_1H_7$ | 108.3 | 108.8 | 108.0 | 109.0 | 107.3 |
| $\angle C_2Sn_1H_8$ | 110.4 | 110.4 | 110.4 | 110.4 | 110.7 |
| $\angle H_7Sn_1H_8$ | 109.7 | 109.3 | 109.8 | 109.2 | 109.8 |
| | | | Dihedral Angles | | |
| $\angle C_3C_2Sn_1H_7$ | 0.0 | 180.0 | 0.0 | 180.0 | 0.0 |
| $\angle C_3C_2Sn_1H_8$ | −120.2 | 60.1 | −120.1 | 60.0 | −119.8 |
| | | | Energy[c] | | |
| $E_0$ | −292.48425 | −292.48302 | −294.10866 | −294.10750 | −293.03862 |
| | | | Relative Energy[d] | | |
| $\Delta E$ | 0.0 | 3.23 | 0.0 | 3.04 | |

[a] Distances in pm, angles in deg, energy in hartree, rotational barrier, $\Delta E$, in kJ mol$^{-1}$. [b] The following basis sets were used: cc-pVTZ for C and H atoms and cc-pVTZ-PP for the Sn atom. The frozen-core procedure was employed. [c] In hartree and corrected for zero-point vibrational energies. [d] Relative to the *sp* form.

used in the least-squares structure analysis. The raw data were further processed as described elsewhere.[16]

The necessary modification and scattering functions were computed from tabulated atomic scattering factors[17] for the proper wavelength and *s*-values. The experimental backgrounds were computed using the program KCED12,[18] where the coefficients of a chosen degree of a polynomial function are determined by the least-squares method by minimizing the differences between the total experimental intensity and the molecular intensity calculated from the current best geometrical model. The average experimental intensities were modified by $s/|f'_C f'_{Ge}|$, where $f'$ denotes the coherent scattering factors. The experimental conditions employed in the GED experiments are given in Table 1.

## Quantum Chemical Calculations

**Procedure.** Quantum chemical calculations were performed for vinyl- and allylstannane using the GAUSSIAN03 suite of programs[19] running on the HP "superdome" facilities in Oslo. Full geometry optimizations were carried out for the *sp* and *ap* forms of vinylstannane (Figure 1) and of each of the *sp*, *ap*, and *ac* forms of allylstannane (Figure 2) at the ab initio Hartree−Fock (HF) level of theory, followed by density functional theory calculations at the B3LYP level.[20,21] Dunning's correlation-consistent polarized valence triple-$\zeta$ (cc-pVTZ) basis set[22] was employed for the carbon and hydrogen atoms, whereas the cc-pVTZ-PP basis set[23] was used for the tin atom. This basis set includes a small-core relativistic pseudopotential to replace 28 core electrons ([Ar] + 3d).[24] Vibrational frequencies were calculated in each case.

It has been claimed that Møller−Plesset second-order perturbation calculations (MP2) using a comparatively large basis set will predict structures that are close to the equilibrium structures.[25] MP2 frozen core (FC) calculations using the same

(16) Gundersen, S.; Samdal, S.; Seip, R.; Strand, T. G. *J. Mol. Struct.* **2004**, *691*, 149.
(17) Ross, A. W.; Fink, M.; Hilderbrandt, R. *International Tables for Crystallography*; Kluwer Academic Publishers: Dordrecht, 1992.
(18) Gundersen, G.; Samdal, S. Annual Report 1976 from the Norwegian GED Group, 1976.
(19) Frisch, M. J.; Trucks, G. W.; Schlegel, H. B.; Scuseria, G. E.; Robb, M. A.; Cheeseman, J. R.; Montgomery, J. A., Jr.; Vreven, T.; Kudin, K. N.; Burant, J. C.; Millam, J. M.; Iyengar, S. S.; Tomasi, J.; Barone, V.; Mennucci, B.; Cossi, M.; Scalmani, G.; Rega, N.; Petersson, G. A.; Nakatsuji, H.; Hada, M.; Ehara, M.; Toyota, K.; Fukuda, R.; Hasegawa, J.; Ishida, M.; Nakajima, T.; Honda, Y.; Kitao, O.; Nakai, H.; Klene, M.; Li, X.; Knox, J. E.; Hratchian, H. P.; Cross, J. B.; Adamo, C.; Jaramillo, J.; Gomperts, R.; Stratmann, R. E.; Yazyev, O.; Austin, A. J.; Cammi, R.; Pomelli, C.; Ochterski, J. W.; Ayala, P. Y.; Morokuma, K.; Voth, G. A.; Salvador, P.; Dannenberg, J. J.; Zakrzewski, V. G.; Dapprich, S.; Daniels, A. D.; Strain, M. C.; Farkas, O.; Malick, D. K.; Rabuck, A. D.; Raghavachari, K.; Foresman, J. B.; Ortiz, J. V.; Cui, Q.; Baboul, A. G.; Clifford, S.; Cioslowski, J.; Stefanov, B. B.; Liu, G.; Liashenko, A.; Piskorz, P.; Komaromi, I.; Martin, R. L.; Fox, D. J.; Keith, T.; Al-Laham, M. A.; Peng, C. Y.; Nanayakkara, A.; Challacombe, M.; Gill, P. M. W.; Johnson, B.; Chen, W.; Wong, M. W.; Gonzalez, C.; Pople, J. A. *Gaussian 03*, Revision B.03; Gaussian, Inc.: Pittsburgh, PA, 2003.
(20) Becke, A. D. *J. Chem. Phys.* **1993**, *98*, 5648.
(21) Lee, C.; Yang, W.; Parr, R. G. *Phys. Rev. B* **1988**, *37*, 785.
(22) Dunning, T. H., Jr. *J. Chem. Phys.* **1989**, *90*, 1007.
(23) Peterson, K. A. *J. Chem. Phys.* **2003**, *119*, 11099.
(24) Metz, B.; Stoll, H.; Dolg, M. *J. Chem. Phys.* **2000**, *113*, 2563.

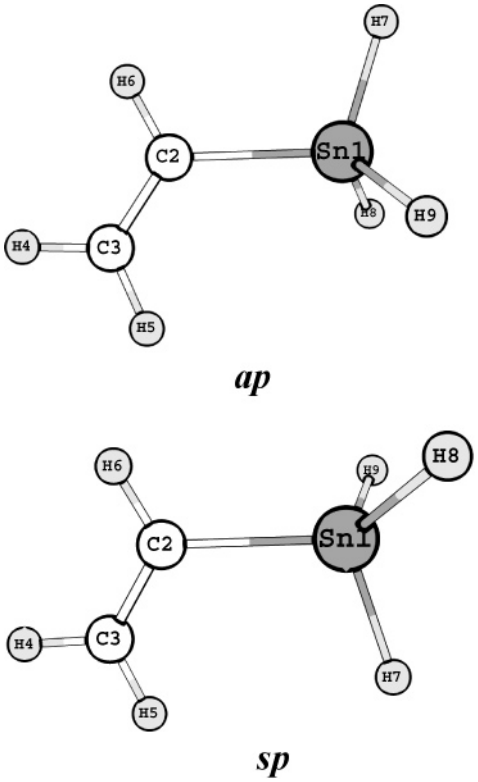


**Figure 1.** The *antiperiplanar* (*ap*) and *synperiplanar* (*sp)* rotamers of vinylstannane. The *sp* rotamer is the only stable form of this molecule.

basis sets were performed for the most stable rotamers of vinyl- and allylstannane only, owing to restrictions on computer time.

Selected results are listed in Tables 2 and 3. The energies shown in these tables are total electronic energies, which have been corrected for zero-point vibrational energies. The B3LYP and MP2 vibrational frequencies and their assignments are shown in Tables 4 and 5. Vibrational frequencies have been reported for the gas-phase infrared spectrum of vinylstannane.[4,5] They are included in Table 4. The gas-phase spectrum of allylstannane is listed in Table 5. This spectrum was obtained at room temperature and a pressure of 50 mbar using a Nicolet Avatar 320 FT-IR spectrometer having a resolution of 0.5 $cm^{-1}$.

**Vinylstannane.** Some comments are warranted. The *sp* form of vinylstannane was found to be more stable than the *ap* conformation. The HF energy difference between *sp* and the *ap* form is 3.2 kJ $mol^{-1}$, and nearly the same value, 3.0 kJ $mol^{-1}$, is found in the B3LYP calculations. No imaginary vibrational frequencies were computed for the *sp* form as opposed to the *ap* rotamer, which was found to have *one* imaginary frequency associated with rotation of the $SnH_3$ group around the $Sn_1-C_2$ bond. The *sp* form is therefore a minimum on the energy hypersurface, whereas the *ap* form is a first-order transition state.[26] The energy difference of the two forms (about 3 kJ $mol^{-1}$) corresponds to the rotational barrier of the stannyl group.

It should be noted that the MP2 structural parameters of the *sp* isomer are close to those computed using the B3LYP or HF procedures, apart from the $Sn_1-C_2$ bond length, which is predicted to be significantly shorter (2−4 pm) in the MP2 calculations than in the HF or the B3LYP calculations.

(25) Helgaker, T.; Gauss, J.; Jørgensen, P.; Olsen, J. *J. Chem. Phys.* **1997**, *106*, 6430.

(26) Hehre, W. J.; Radom, L.; Schleyer, P. v. R. *Ab Initio Molecular Orbital Theory*; John Wiley & Sons: New York, 1986.

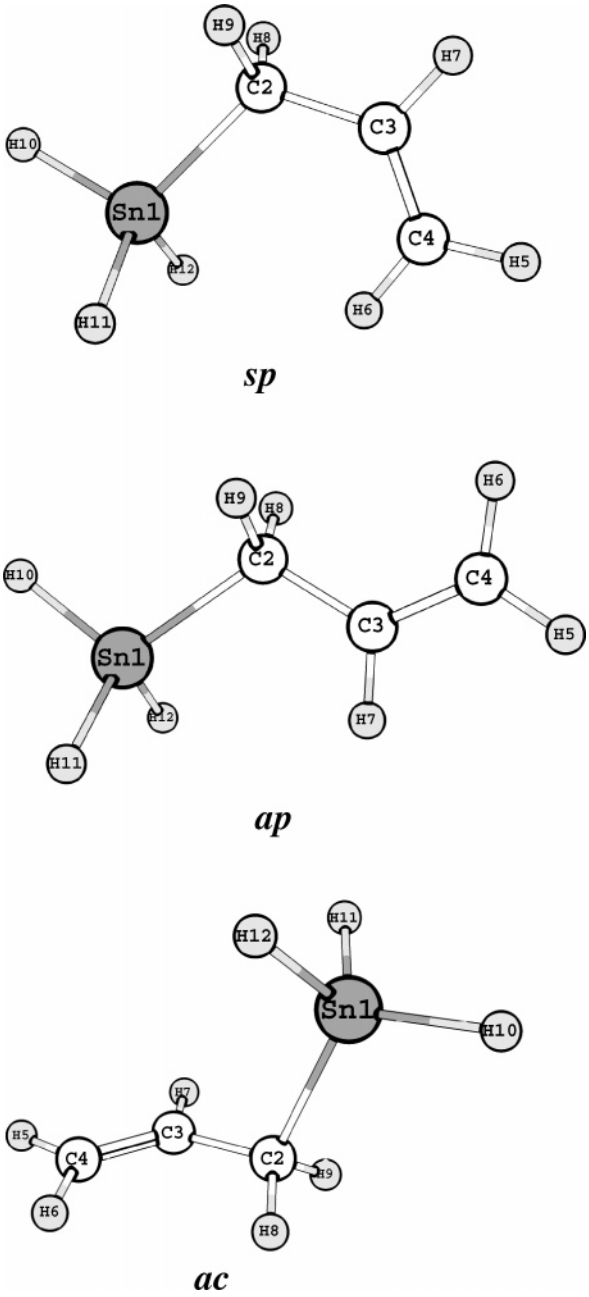


**Figure 2.** The *synperiplanar* (*sp*), *antiperiplanar* (*ap*), and *anticlinal* (*ac*) conformers of allylstannane with atom numbering. The gas phase consists almost exclusively of *ac* at room temperature.

The principal inertial axis dipole moment components of the *sp* rotamer were calculated to be $\mu_a = 0.11$, $\mu_b = 0.63$, and $\mu_c = 0.0$ D (by symmetry) by the MP2 procedure. Similar results were obtained in the HF and B3LYP calculations. The comparatively small calculated dipole moment components are consistent with the failure to observe a microwave spectrum (see above), taking into consideration that the calculated dipole moments are normally larger than their experimental counterparts.

**Allylstannane.** The *ac* isomer was determined to be the global energy minimum in the case of allylstannane. No imaginary vibrational frequencies were calculated in this case. A different situation was found for the *ap* form. One imaginary frequency associated with the rotation around the $C_2-C_3$ bond was obtained for this conformation, which is therefore a transition state. The *sp* rotamer is another stable conformation, since no

**Table 3. Calculated Structure[a] of Allylstannane**

| | HF[b] | | | B3LYP[b] | | | MP2(FC)[b] |
|---|---|---|---|---|---|---|---|
| | $C_s$ *sp* | $C_s$ *ap* | $C_1$ *ac* | $C_s$ *sp* | $C_s$ *ap* | $C_1$ *ac* | $C_1$ *ac* |
| | | | | Bond Lengths | | | |
| $Sn_1-C_2$ | 216.4 | 216.2 | 217.3 | 217.8 | 217.5 | 219.3 | 214.7 |
| $C_2-C_3$ | 150.4 | 151.5 | 149.4 | 149.8 | 151.1 | 148.6 | 148.8 |
| $C_3=C_4$ | 131.6 | 131.6 | 131.8 | 132.7 | 132.7 | 133.1 | 133.7 |
| $Sn_1-H_{10}$ | 171.5 | 171.3 | 171.5 | 171.8 | 171.6 | 171.9 | 169.3 |
| $Sn_1-H_{11}$ | 171.3 | 171.5 | 171.4 | 171.6 | 171.8 | 171.7 | 169.2 |
| $Sn_1-H_{12}$ | 171.3 | 171.5 | 171.2 | 171.6 | 171.8 | 171.5 | 169.0 |
| $C_2-H_8$ | 108.6 | 108.4 | 108.4 | 109.3 | 109.1 | 108.9 | 108.9 |
| $C_2-H_9$ | 108.6 | 108.4 | 108.3 | 109.3 | 109.1 | 109.0 | 108.9 |
| $C_3-H_7$ | 107.9 | 107.7 | 107.8 | 108.9 | 108.6 | 108.7 | 108.6 |
| $C_4-H_5$ | 107.4 | 107.4 | 107.3 | 108.2 | 108.2 | 108.1 | 108.0 |
| $C_4-H_6$ | 107.4 | 107.4 | 107.5 | 108.2 | 108.2 | 108.4 | 108.2 |
| | | | | Bond Angles | | | |
| $\angle Sn_1C_2C_3$ | 118.6 | 115.2 | 112.5 | 118.0 | 115.0 | 111.8 | 109.8 |
| $\angle C_2C_3C_4$ | 127.9 | 124.4 | 125.8 | 127.8 | 124.3 | 125.8 | 125.1 |
| $\angle C_3C_2H_8$ | 109.2 | 110.2 | 110.7 | 109.9 | 110.8 | 112.0 | 111.3 |
| $\angle C_3C_2H_9$ | 109.2 | 110.2 | 111.2 | 109.9 | 110.8 | 111.8 | 111.6 |
| $\angle C_3C_4H_5$ | 121.0 | 121.2 | 121.2 | 121.2 | 121.4 | 121.4 | 121.2 |
| $\angle C_3C_4H_6$ | 121.0 | 121.2 | 121.8 | 121.2 | 121.4 | 121.7 | 121.1 |
| $\angle C_4C_3H_7$ | 117.5 | 117.5 | 118.3 | 117.6 | 117.6 | 118.4 | 118.4 |
| $\angle Sn_1C_2H_8$ | 106.8 | 107.2 | 106.9 | 106.4 | 106.7 | 106.8 | 108.0 |
| $\angle Sn_1C_2H_9$ | 106.8 | 107.2 | 107.5 | 106.4 | 106.7 | 105.7 | 107.6 |
| $\angle C_2Sn_1H_{10}$ | 107.5 | 109.7 | 109.7 | 107.5 | 109.8 | 110.1 | 111.1 |
| $\angle C_2Sn_1H_{11}$ | 111.4 | 110.1 | 109.8 | 111.4 | 110.0 | 109.6 | 108.9 |
| $\angle C_2Sn_1H_{12}$ | 111.4 | 110.1 | 109.7 | 111.4 | 110.0 | 109.3 | 108.4 |
| $\angle H_{10}Sn_1H_{11}$ | 108.8 | 109.2 | 109.0 | 108.7 | 109.2 | 109.1 | 109.3 |
| $\angle H_{10}Sn_1H_{12}$ | 108.8 | 109.2 | 109.3 | 108.7 | 109.2 | 109.5 | 109.7 |
| $\angle H_{11}Sn_1H_{12}$ | 108.9 | 108.6 | 109.3 | 108.9 | 108.6 | 109.3 | 109.5 |
| $\angle H_8C_2H_9$ | 105.3 | 106.4 | 107.8 | 105.3 | 106.4 | 108.5 | 108.4 |
| | | | | Dihedral Angles | | | |
| $\angle C_4C_3C_2Sn_1$ | 0.0 | 180.0 | 106.8 | 0.0 | 180.0 | 105.7 | 103.7 |
| $\angle C_3C_2Sn_1H_{10}$ | 180.0 | 180.0 | 171.9 | 180.0 | 180.0 | 171.9 | 172.3 |
| $\angle C_3C_2Sn_1H_{11}$ | 60.9 | 59.9 | 52.1 | 60.9 | 59.8 | 52.0 | 52.0 |
| $\angle C_3C_2Sn_1H_{12}$ | −60.9 | −59.9 | −68.1 | −60.9 | −59.8 | −67.8 | −67.1 |
| $\angle C_2C_3C_4H_5$ | 180.0 | 180.0 | −178.9 | 180.0 | 180.0 | −178.9 | −178.1 |
| $\angle C_2C_3C_4H_6$ | 0.0 | 0.0 | 1.2 | 0.0 | 0.0 | 1.2 | 2.0 |
| $\angle H_5C_4C_3H_7$ | 0.0 | 0.0 | 0.0 | 0.0 | 0.0 | −0.1 | −0.3 |
| | | | | Energy[c] | | | |
| $E_0$ | −331.50187 | −331.49913 | −331.50567 | −333.41036 | −333.40751 | −333.41431 | −332.23750 |
| | | | | Relative Energy[d] | | | |
| $\Delta E$ | 10.0 | 17.2 | 0.0 | 10.4 | 17.2 | 0.0 | 0.0 |
| $\Delta G^0$ | 9.0 | *e* | 0.0 | 6.1 | *e* | 0.0 | 0.0 |

[a] Distances in pm, angles in deg, energy in hartree, rotational barrier, $\Delta E$, in kJ mol$^{-1}$. [b] The following basis sets were used: cc-pVTZ for C and H atoms and cc-pVTZ-PP for Sn atoms. The frozen-core procedure was employed. [c] Corrected for vibrational ZPE. [d] Relative to the energy of the *ac* conformer. Dimension: kJ/mol. [e] Not calculated.

imaginary frequencies were predicted for it. However, its total energy is significantly *higher* than that of the *ac* form. It is seen in Table 3 that the *ac* form is predicted by both HF and B3LYP calculations to be more stable than the *sp* by about 10 kJ/mol, whereas the *ap* transition state is predicted to be about 17 kJ/mol above the *ac* conformer.

The Gibbs energy differences between the *ap* and *ac* rotamers, $\Delta G°$, which are given in the same table, were calculated to be 9.9 and 6.1 kJ/mol, respectively. The difference between these two numbers (9.9 and 6.1) is mainly due to a vibrational entropy effect. The lowest torsional frequency is predicted to be 18 cm$^{-1}$ for the *sp* rotamer and 81 cm$^{-1}$ for the *ac* rotamer in the B3LYP calculations, while 66 cm$^{-1}$ for the *sp* rotamer and 84 cm$^{-1}$ for the *ac* rotamer were computed for the HF calculations.

The potential energy function for internal rotation about the C−Sn bond, which was calculated at the B3LYP level of theory, is sketched in Figure 3. The energy of the *ac* conformer has been arbitrarily taken to be zero. Calculations were performed at intervals of 15°, with full optimization of all the other structural parameters.

It is noted that the $Sn_1-C_2$ bond length is considerably shorter in the MP2 calculations than in the HF and B3LYP calculations, just as found for vinylstannane. Moreover, the $\angle C_2C_3C_4$ and $\angle Sn_1C_2C_3$ bond angles in the *sp* conformation are calculated to be about 2° and 6° larger than in the *ac* conformation. This may reflect steric strain arising when the vinyl and stannyl groups are brought into close proximity.

## Structure Refinement

**Vinylstannane.** It was found in the quantum chemical calculations above that the *sp* isomer with a symmetry plane ($C_s$ symmetry) is the only stable form of this compound. Fifteen independent parameters were chosen to describe its molecular structure. These parameters are the bond distances $r(Sn_1C_2)$, $r(C_2C_3)$, $r(C_2H_6)$, $r(C_3H_4)$, $r(C_3H_5)$, $r(Sn_1H_7)$, and $r(Sn_1H_8) = r(Sn_1H_9)$ and the bond angles $\angle Sn_1C_2C_3$, $\angle C_2C_3H_4$, $\angle C_2C_3H_5$, $\angle C_3C_2H_6$, $\angle C_2Sn_1H_7$, $\angle C_2Sn_1H_8 = \angle C_2Sn_1H_9$, and $\angle H_7Sn_1H_8 = \angle H_7Sn_1H_9$. In addition, the $\angle C_3C_2Sn_1H_7$ dihedral angle was allowed to vary in order to test whether the rotational barrier of the stannyl group could be determined by electron diffraction.

**Table 4. Calculated Fundamental Frequencies and Tentative Assignments[a] for the *sp* Rotamer of Vinylstannane**

| symmetry | | B3LYP | MP2(FC) | IR (gas) |
|---|---|---|---|---|
| A″ | C−$SnH_3$ *tor* | 90 | 110 | |
| A′ | SnCC *b* | 225 | 228 | |
| A″ | $SnH_3$ *r* | 364 | 379 | |
| A′ | Sn−C *st* | 439 | 469 | |
| A′ | $SnH_3$ *r* | 548 | 577 | |
| A″ | CH *w* | 562 | 580 | |
| A′ | $SH_3$ *s b* | 689 | 726 | 683[b] |
| A″ | $SH_3$ *as b* | 717 | 760 | 693[b] |
| A′ | $SH_3$ *as b* | 727 | 771 | 717[b] |
| A″ | $CH_2$ *w* | 993 | 995 | 953[b] |
| A′ | $CH_2$ *r* | 1016 | 1017 | 1002[b] |
| A″ | CH *w* | 1043 | 1060 | 1008[b] |
| A′ | CH *r* | 1283 | 1288 | 1250[c] |
| A′ | $CH_2$ *sc* | 1440 | 1446 | |
| A′ | C═C *st* | 1650 | 1637 | ca. 1600[b] |
| A′ | $SnH_3$ *s st* | 1893 | 2034 | |
| A″ | $SnH_3$ *as st* | 1893 | 2038 | 1865[c] |
| A′ | $SnH_3$ *as st* | 1902 | 2040 | |
| A′ | $CH_2$ *s st* | 3100 | 3152 | 2938[c] |
| A′ | CH *st* | 3127 | 3183 | 2980[c] |
| A′ | $CH_2$ *as st* | 3177 | 3243 | 3042[c] |

[a] Frequencies in $cm^{-1}$; *tor*, torsion; *b*, bending; *st*, stretching; *w*, wagging; *tw*, twist; *sc*, scissoring; *r*, rock; *s*, symmetric; *as*, asymmetric. [b] Ref 4. [c] Ref 5.

**Table 5. Calculated Fundamental Frequencies and Tentative Assignments for the *ac* Rotamer of Allylstannane[a]**

| assignment | B3LYP | MP2(FC) | IR (gas)[b] |
|---|---|---|---|
| C−Sn *tor* | 81 | 79 | |
| C−C *tor* | 96 | 95 | |
| C−C−Sn *b* | 194 | 194 | |
| C═C−C *b* | 377 | 388 | |
| $SnH_3$ *r* | 412 | 418 | |
| $SnH_3$ r | 433 | 450 | |
| Sn−C *st* | 491 | 521 | |
| $SnH_3$ *s b* | 685 | 708 | 677 |
| $=CH_2$ *tw* | 702 | 718 | |
| $SnH_3$ *as b* | 720 | 755 | |
| $SnH_3$ *as b* | 727 | 762 | |
| $=CH_2$ *r* | 786 | 784 | |
| $=CH_2$ *w* | 928 | 916 | 901 |
| C−C *st* | 945 | 954 | 991 |
| $=CH_2$ *r* | 1023 | 1024 | 1027 |
| =CH *w* | 1060 | 1058 | |
| $CH_2$ *w* | 1136 | 1142 | 1018 |
| $CH_2$ *w* | 1219 | 1224 | 1194 |
| =CH *b* | 1335 | 1327 | |
| $=CH_2$ *sc* | 1444 | 1441 | |
| $CH_2$ *sc* | 1474 | 1473 | |
| C═C *st* | 1690 | 1685 | 1634 |
| $SnH_3$ *s st* | 1881 | 2027 | 1904 |
| $SnH_3$ *as st* | 1895 | 2034 | |
| $SnH_3$ *as st* | 1905 | 2039 | |
| $CH_2$ *s st* | 3049 | 3094 | 3091 |
| $CH_2$ *as st* | 3098 | 3156 | |
| =CH *st* | 3123 | 3174 | |
| $=CH_2$ *s st* | 3131 | 3183 | |
| $=CH_2$ *as st* | 3215 | 3279 | |

[a] See Table 4 for abbreviations. [b] See text.

The low scattering power of the hydrogen atoms was the reason for using constraints as follows: $r(C_3H_4) = r(C_2H_6) + \Delta1$, where $\Delta1$ is the difference between the bond lengths $r(C_3H_4)$ and $r(C_2H_6)$. Similarly, $r(C_3H_5) = r(C_2H_6) + \Delta2$, $r(Sn_1H_8) = r(Sn_1H_9) = r(Sn_1H_7) + \Delta3$, $\angle C_2C_3H_4 = \angle C_3C_2H_6 + \Delta4$, $\angle C_2C_3H_5 = \angle C_3C_2H_6 + \Delta5$, $\angle C_2Sn_1H_8 = \angle C_2Sn_1H_9 = \angle C_2Sn_1H_7 + \Delta6$, $\angle H_7Sn_1H_8 = \angle H_7Sn_1H_9 = \angle C_2Sn_1H_7 + \Delta7$. The differences, $\Delta1-7$, were taken from the quantum chemical calculation (B3LYP//cc-pVTZ-PP(Sn)/cc-pVTZ(C,H)). They are 0.02, −0.13, and 0.14 pm and 3.08°, 3.77°, 2.39°, and 1.78°, respectively. It was not possible to determine $\angle C_3C_2H_6$. This angle was therefore fixed at the value shown in Table 6.

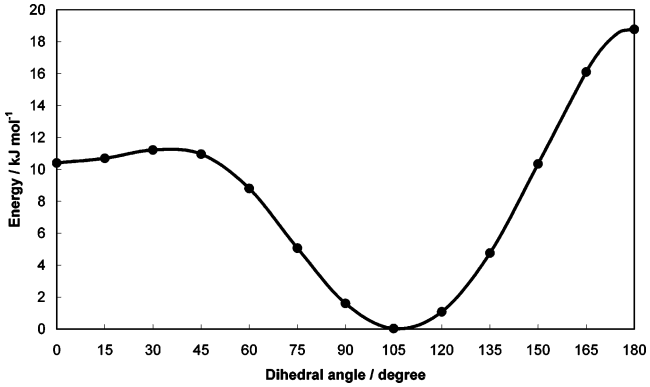


**Figure 3.** B3LYP potential energy function for rotation about the C−Sn bond in allylstannane. Calculations were performed at intervals of 15°, shown as dots in the figure. 0° corresponds to the *sp* conformer and 106° to the *ac* conformer.

**Table 6. Structure and *u*-Values of Vinylstannane[a,b]**

| | $r_a$ | $u_{calc}$ | $u_{exp}$ |
|---|---|---|---|
| | Bond Lengths | | |
| $Sn_1-C_2$ | 215.1(6) | 5.1 | 6.3(6) |
| $C_2=C_3$ | 133.7(5) | 4.0 | 4.0 |
| $Sn_1-H_7$ | 180.4(9) | 9.2 | 10.7(10) |
| $Sn_1-H_8$[c] | 180.5(9) | 9.2 | 10.7(10) |
| $C_2-H_6$ | 108.4(8) | 7.5 | 7.5 |
| $C_3-H_4$[c] | 108.4(8) | 7.4 | 7.4 |
| $C_3-H_5$[c] | 108.2(8) | 7.4 | 7.4 |
| | Bond Angles | | |
| $\angle Sn_1C_2C_3$ | 121.6(4) | | |
| $\angle C_3C_2H_6$[d] | 118.8 | | |
| $\angle C_2C_3H_4$[c] | 121.8 | | |
| $\angle C_2C_3H_5$[c] | 122.5 | | |
| $\angle C_2Sn_1H_7$ | 106.3(24) | | |
| $\angle C_2Sn_1H_8$[c] | 108.7 | | |
| $\angle H_7Sn_1H_8$[c] | 108.1 | | |
| | Dihedral Angle | | |
| $\angle C_3C_2Sn_1H_7$ | 9(31) | | |
| | $R_f$, %= 9.91[e] | | |

[a] Distances and *u*-values in pm, angles and dihedral angles in deg. Parenthesized values are estimated error limits given as $2.5(\sigma^2_{lsq} + (0.001r)^2)^{1/2}$ for bond distances where $\sigma_{lsq}$ is one standard deviation obtained from the least-squares refinements using a diagonal weight matrix and the second term represent 0.1% uncertainty in the electron wavelength. For angles and *u*-values the estimated error limits are $2.5\sigma_{lsq}$. The error estimates are in units of the last digits. [b] The B3LYP structure that was used as the starting point in least-squares analysis; see text. [c] These parameters were calculated according to the constraints discussed in the text. [d] Fixed. [e] Goodness of fit defined as $\sum_s w(I_s^{obs} - I_s^{calc})^2/\sum_s w(I_s^{obs})^2$, where *w* is a weight function usually equal to 1.

An attempt was made to determine the barrier to internal rotation of the $SnH_3$ group. The $C_3C_2Sn_1H_7$ dihedral angle was refined for this purpose. A value of 9° with one standard deviation of 13° was found in this refinement. Clearly, the scattering from $C_3\cdots H_{Sn}$ pairs of atoms is not sufficient to obtain an accurate value for the barrier to internal rotation of the stannyl group. Fixing this dihedral angle at 0.0° did not influence the values of the other structural parameters.

The root-mean-square vibrational amplitudes (*u*-values) and perpendicular correction coefficients (*D*-values) were calculated employing the ASYM program[27,28] using the B3LYP//cc-pVTZ-PP(Sn)/cc-pVTZ(C,H) force fields. Vibrational amplitudes for

(27) Hedberg, L.; Mills, I. M. *J. Mol. Spectrosc.* **1993**, *160*, 117.
(28) Hedberg, L.; Mills, I. M. *J. Mol. Spectrosc.* **2000**, *203*, 82.

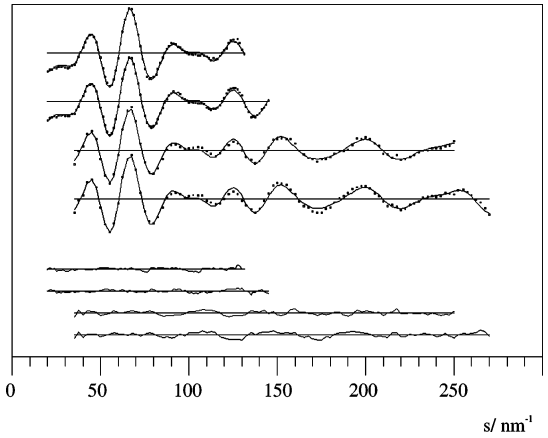


**Figure 4.** Intensity curves for vinylstannane. The two upper cruves are for the *y*- and *x*-directions of the long camera distance, respectively. The two next curves are for the *y*- and *x*-directions of the middle camera distance. The four lower curves are difference curves. Camera distances are found in Table 1.

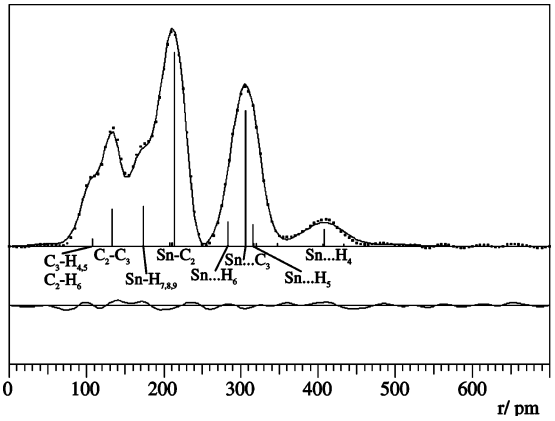


**Figure 5.** Radial distribution curve for vinylstannane (upper curve) and difference curve (lower curve).

distances with small contributions to the total molecular scattering were kept at the theoretical values, whereas the other *u*-values were refined with the result shown in Table 6. The B3LYP structure was used as the starting point in the structure refinement. The KCED25 least-squares fitting program[29] was used. The intensity and radial distribution curves are shown in Figures 5 and 7, while the experimental structure is shown in Table 6.

**Allylstannane.** The gas phase was initially assumed to contain a mixture of the *ac* and *sp* forms. However, the first analysis revealed that the *sp* form could not be detected in the gas at room temperature. A crude estimate of the composition of the gas phase was therefore calculated using the theoretical Gibbs energy difference, $\Delta G°$, between the *sp* and *ac* forms shown in Table 3. Considering the equilibrium *ac* ↔ *sp*, the equilibrium constant $K = N_{sp}/N_{ac} = \sigma_{sp}X_{sp}/\sigma_{ac}X_{ac} = X_{sp}/2X_{ac}$ where $\sigma$ is the statistical weight and $X$ is the mole fraction. $\Delta G° = -RT \ln K$ at equilibrium, where $R$ is the universal gas constant and $T$ the absolute temperature. The statistical weight of *ac* has been assumed to be twice the statistical weight of *sp*. The mole fraction of the *ac* conformer was calculated to be 0.97 at room temperature using the HF results and 0.86 employing the B3LYP calculations. The final structural analysis was performed assuming that only the *ac* rotamer is present in the gas at room

(29) Gundersen, G.; Samdal, S.; Seip, H.-M.; Strand, T. G. Annual Report 1977, 1980, 1981 from the Norwegian Gas Electron Diffraction Group.

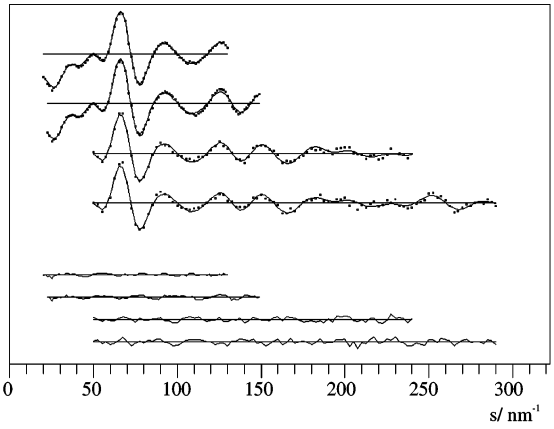


**Figure 6.** Intensity curves for allylstannane. Same definitions as for vinylstannane; see Figure 4.

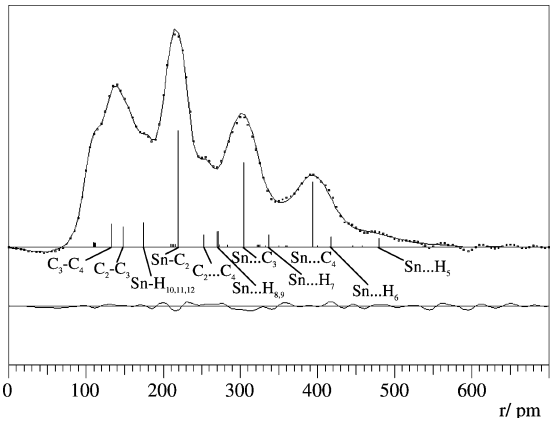


**Figure 7.** Radial distribution (upper) and difference (lower) curves for allylstannane.

temperature. The possible existence of a small fraction of the *sp* form is not expected to have any influence on the results.

The following structural parameters were chosen as independent: the bond lengths $r(Sn_1C_2)$, $r(C_2C_3)$, $r(C_3C_4)$, $r(C_4H_5)$, $r(C_4H_6)$, $r(C_3H_7)$, $r(C_2H_8)$, $r(C_2H_9)$, $r(Sn_1H_{10})$, $r(Sn_1H_{11})$, and $r(Sn_1H_{12})$, the bond angles $\angle Sn_1C_2C_3$, $\angle C_2C_3C_4$, $\angle C_4C_3H_7$, $\angle C_3C_4H_5$, $\angle C_3C_4H_6$, $\angle C_3C_2H_8$, $\angle C_3C_2H_9$, $\angle Sn_1C_2H_8$, $\angle Sn_1C_2H_9$, $\angle C_2Sn_1H_{10}$, $\angle C_2Sn_1H_{11}$, $\angle C_2Sn_1H_{12}$, $\angle H_{10}Sn_1H_{11}$, and $\angle H_{10}Sn_1H_{12}$, and the dihedral angles $\angle C_4C_3C_2Sn_1$, $\angle C_2C_3C_4H_5$, $\angle C_2C_3C_4C_6$, $\angle H_6C_4C_3H_7$, and $\angle C_3C_2Sn_1H_{10}$. The last three dihedral angles were fixed at 0° or 180° (see Figure 2), while the first was refined. The following constraints were used in the structure determination: $r(C_4H_6) = r(C_4H_5) + \Delta 1$, $r(C_3H_7) = r(C_4H_5) + \Delta 2$, $r(C_2H_8) = r(C_4H_5) + \Delta 3$, $r(C_2H_9) = r(C_4H_5) + \Delta 4$, $r(Sn_1H_{11}) = r(Sn_1H_{10}) + \Delta 5$, $r(Sn_1H_{12}) = r(Sn_1H_{10}) + \Delta 6$, $\angle C_3C_4H_6 = \angle C_3C_4H_5 + \Delta 7$, $\angle C_4C_3H_7 = \angle C_3C_4H_5 + \Delta 8$, $\angle C_3C_2H_9 = \angle C_3C_2H_8 + \Delta 9$, $\angle Sn_1C_2H_9 = \angle Sn_1C_2H_8 + \Delta 10$, $\angle C_2Sn_1H_{11} = \angle C_2Sn_1H_{10} + \Delta 11$, $\angle C_2Sn_1H_{12} = \angle C_2Sn_1H_{10} + \Delta 12$, $\angle H_{10}Sn_1H_{11} = \angle C_2Sn_1H_{10} + \Delta 13$, $\angle H_{10}Sn_1H_{12} = \angle C_2Sn_1H_{10} + \Delta 14$. The differences (the $\Delta$'s) were those calculated by the B3LYP//cc-pVTZ-PP(Sn)/cc-pVTZ(C,H) procedure. They are 0.25, 0.54, 0.82, 0.91, −0.22, and −0.40 pm and 0.30°, −3.06°, −0.19°, −1.05°, −0.51°, −0.83°, −1.04°, and −0.63°, respectively.

The *u*- and *D*-values were derived in the same way as that described previously for vinylstannane. The refinements were carried out in the same manner as for vinylstannane. The

**Table 7. Structure and *u*-Values of Allylstannane[a,b]**

| | $r_a$ | $u_{calc}$ | $u_{exp}$ |
|---|---|---|---|
| | Bond Lengths | | |
| $Sn_1-C_2$ | 218.9(8) | 5.8 | 6.0(8) |
| $C_2-C_3$ | 148.1(10) | 5.0 | 5.8(11) |
| $C_3=C_4$ | 132.9(7) | 4.1 | 4.0(9) |
| $Sn_1-H_{10}$ | 174.9(13) | 9.5 | 11.5(14) |
| $Sn_1-H_{11}$[c] | 174.7(13) | 9.5 | 11.4(14) |
| $Sn_1-H_{12}$[c] | 174.5(13) | 9.4 | 11.4(14) |
| $C_2-H_8$[c] | 111.4(6) | 7.7 | 7.7 |
| $C_2-H_9$[c] | 111.5(6) | 7.7 | 7.7 |
| $C_3-H_7$[c] | 109.6(6) | 7.6 | 7.6 |
| $C_4-H_5$ | 110.5(6) | 7.6 | 7.6 |
| $C_4-H_6$[c] | 110.8(6) | 7.6 | 7.6 |
| | Bond Angles | | |
| $\angle Sn_1C_2C_3$ | 110.9(6) | | |
| $\angle C_2C_3C_4$ | 128.5(16) | | |
| $\angle C_3C_2H_8$ | 112.0 | | |
| $\angle C_3C_2C_9$[c] | 111.8 | | |
| $\angle C_3C_4H_5$ | 121.4 | | |
| $\angle C_3C_4H_6$[c] | 121.7 | | |
| $\angle C_4C_3H_7$[c] | 118.4 | | |
| $\angle Sn_1C_2H_8$ | 106.8 | | |
| $\angle Sn_1C_2H_9$ | 105.7 | | |
| $\angle C_2Sn_1H_{10}$ | 111.8(35) | | |
| $\angle C_2Sn_1H_{11}$[c] | 111.3 | | |
| $\angle C_2Sn_1H_{12}$[c] | 111.0 | | |
| $\angle H_{10}Sn_1H_{11}$[c] | 110.7 | | |
| $\angle H_{10}Sn_1H_{12}$[c] | 111.2 | | |
| | Dihedral Angle | | |
| $\angle C_4C_3C_2Sn_1$ | 102.9(19) | | |
| | $R_f = 12.6\%$ | | |

[a−c] Same comments as for Table 6.

intensity and radial distribution curves for the final model are shown in Figures 5 and 7. The experimental structure is given in Table 7.

## Discussion

The $r_a$ value of the prototype C(sp$^2$)−Sn(IV) bond length in vinylstannane is 215.1(6) pm (Table 6). The equilibrium bond length, $r_e$, can be estimated using $r_e \approx r_a + u^2/r_a - K - \delta r - 1.5au$,[2,30,31] where $u$ is the root-mean-square amplitude of vibration, $K$ is the perpendicular correction coefficient, $\delta r$ is the centrifugal stretching, and $a$ is the Morse anharmonicity parameter. Using the SHRINK program,[32,33] the anharmonicity parameter was calculated by Sipachev[34] to be $a = 0.0162$ pm$^{-1}$ for a C−Sn bond. The centrifugal stretching, $\delta r$, which usually is very small, is calculated to be 0.13 pm. In this manner, the equilibrium C−Sn bond length is estimated to be $r_e \approx 214.1(6)$ pm in vinylstannane ($K = 0.34$ pm), which should be compared to the MP2(FC) value of 211.2 pm and the B3LYP value of 214.6 pm. The C(sp$^3$)−Sn(IV) bond length in allylstannane ($K = 0.48$ pm) is $r_a = 218.9(8)$ pm, and $r_e$ is estimated to be 217.6(8) pm, which should be compared with the MP2(FC) value of 214.7 pm and the B3LYP value of 219.3 pm. The estimated error in $r_e$ is the experimental error, and since no error related to theory is included, these errors should be considered as lower limits. The C(sp$^2$)−Sn(IV) bond length in allenylstannane[3] ($CH_2$=C=$CHSnH_3$) is $r_a = 213.2(7)$ pm and $r_e = 212.7(7)$ pm, while the MP2(FC) value is 211.7 pm and the B3LYP value is 215.3 pm. The MP2(FC) calculations underestimate the C−Sn bond length, and B3LYP is the preferable method for vinylstannane and allylstannane, but for allenylstannane it is not obvious which method is the best.

Another noticeable feature is that the C(sp$^2$)−Sn(IV) bond length is about 1.9 pm shorter in allenylstannane compared to vinylstannane. A shortening is expected if there is a conjugation in the C=C=C group. However, there is not expected to be any conjugation in the C=C=C group since the two $\pi$-bonds are perpendicular to each other. Actually, both MP2(FC) and B3LYP predict a small increase in the bond length. We do not have a good explanation for this observed shortening. It is also noticeable that the C(sp$^3$)−Sn(IV) bond length is influenced by the substituents to a remarkable degree. The $r_g$ bond length is 214.36(30) pm in tetramethyltin,[35] which is nearly 5 pm shorter than in allylstannane.

Another structural feature of allylstannane is worth noting, viz., the $Sn_1C_2C_3C_4$ dihedral angle, which is 102.9(8)° from *synperiplanar* (0°) in the *ac* conformer. The corresponding $X_1C_2C_3C_4$ dihedral angles, where $X_1$ = C, Si, or Ge, are 119.9(3)°,[36] 106.8(11)°,[37] and 106.2°,[38] respectively. The $X_1C_2C_3C_4$ dihedral angle thus diminishes by as much as 13−17° when the terminal carbon atom in 1-butene ($H_2C$=$CHCH_2CH_3$) is substituted by a heteroatom.

The gaseous composition of this series of allylic compounds is also noticeable. In 1-butene, the *ac* conformation is 0.63(63) kJ mol$^{-1}$ more stable than the *sp* conformation.[36] No *sp* conformation has been found experimentally for the corresponding allylic compounds with heteroatoms ($H_2C$=$CHCH_2XH_3$, X = Si, Ge, Sn).[36−38] The present high-level quantum chemical calculations as well as other recent calculations[38] indicate that the *sp* rotamer in these compounds is 5−8 kJ mol$^{-1}$ less stable than the *ac* conformer.

**Acknowledgment.** We are grateful to Dr. Jean Demaison, Université de Lille 1, for some initial quantum chemical calculations. T.S. thanks the International Student Quota Program of the University of Oslo for financial support. H. V. Volden is acknowledged for recording the electron-diffraction data, and S. Gundersen is acknowledged for workup of the experimental data. We thank Dr. George C. Cole for reading and correcting the manuscript. J.-C.G. thanks the PCMI (INSU-CNRS) for financial support and Dr. Stéphanie Le Serre, who initiated the synthetic work during her Ph.D. studies. A grant from the French-Norwegian Aurora Exchange Program to J.-C.G. and H.M. is gratefully acknowledged. The Research Council of Norway (Programme for Supercomputing) is thanked for a grant of computer time.

OM0601549

(30) Hargittai, I., Hargittai, M., Eds. Stereochemical Applications of Gas-Phase Electron Diffraction, Pt. A: The Electron Diffraction Technique. In *Methods Stereochem. Anal*. **1988**, *10*.
(31) Sim, G. A., Sutton, L. E., Eds. *Specialist Periodical Reports: Molecular Structure by Diffraction Methods*; 1973; Vol. 1.
(32) Sipachev, V. A. *J. Mol. Struct. (THEOCHEM)* **1985**, *22*, 143.
(33) Sipachev, V. A. *J. Mol. Struct.* **2001**, *567−568*, 67.
(34) Sipachev, V. A. *Struct. Chem.* **2000**, *11*, 167.
(35) Nagashima, M.; Fujii, H.; Kimura, M. *Bull. Chem. Soc. Jpn.* **1973**, *46*, 3708.
(36) Kondo, S.; Hirota, E.; Morino, Y. *J. Mol. Spectrosc.* **1968**, *28*, 471.
(37) Imachi, M.; Nakagawa, J.; Hayashi, M. *J. Mol. Struct.* **1983**, *102*, 403.
(38) Horn, A.; Møllendal, H.; Demaison, J.; Petitprez, D.; Moreno, J. R. A.; Benidar, A.; Guillemin, J.-C. *J. Phys. Chem. A* **2005**, *109*, 3822.